Sensors and Materials, Vol. 33, No. 12 (2021) 4623–4641
MYU Tokyo

S & M 2785

Combining ^{137}Cs with GeoWEPP Model to Study Short-term Soil Erosion on Slopes in Karst Areas in Southwestern China

Chuan Yin,[1] Kai Xiong,[2] Hongbing Ji,[3*] and Mingyi Du[1]

[1]Beijing University of Civil Engineering and Architecture, School of Geomatics and Urban Spatial Informatics, Beijing 102616, China
[2]Beijing Municipal Research Institute of Environmental Protection, Beijing 100037, China
[3]University of Science & Technology Beijing, Beijing 100083, China

(Received April 25, 2021; accepted September 7, 2021; online published November 18, 2021)

Keywords: ^{137}Cs, GeoWEPP, soil erosion, karst

The geological and geomorphic environment is complex in karst areas in southwest China, which has seriously hampered the study of soil erosion in these areas. For this reason, the ^{137}Cs tracer method, remote sensing, and Geographic Information System (GIS) technology based on high-precision digital elevation model (DEM) data are used to estimate the soil erosion rate from a point to the surface and for the comprehensive evaluation of the spatial distribution and erosion mechanism of soil erosion on a karst slope. The average ^{137}Cs areal activity of nine sampling sites reached 875 Bq/m^2 (background value of 960 Bq/m^2), the uncultivated land profile of ^{137}Cs was obtained in the topsoil layer of 0–6 cm, and the cultivated land profile of ^{137}Cs was obtained in the topsoil layer of 0–20 cm. The soil erosion intensity in the investigation area was dominated by micro-degree and moderate erosion, and the average soil erosion modulus of uncultivated land was higher than that of cultivated land. The intensity of soil erosion at the slope top was lowest and increased continuously along the slope direction on a hillslope with a short slope and a steep gradient, whereas for a hillslope with a long slope and a low gradient, soil was easily deposited at the slope toe. The area ratio of the slope gradient range of 17–23° was 31.9%, the erosion ratio was 32.2%, and the deposition ratio was 32.9%. On the uncultivated land, the erosion prediction results of the geo-spatial interface for the Water Erosion Prediction Project (GeoWEPP) model were consistent with the estimation results of the ^{137}Cs moving boundary model, but on the cultivated land, the erosion prediction results of the former were larger than those of the latter. Overall, the methodology combining ^{137}Cs and GeoWEPP is favorable for monitoring and assessing regional soil erosion in uncultivated land of a moderately rocky desertification area, but for cultivated land, GeoWEPP gives relatively poor results and must be improved and optimized.

1. Introduction

Soil erosion research is of great significance to regional economic development, environmental ecological protection, and surface material circulation.(1) As the world's largest

*Corresponding author: e-mail: ji.hongbing@hotmail.com
https://doi.org/10.18494/SAM.2021.3418

ISSN 0914-4935

continuous karst zone, the karst areas in southwest China are characterized by geochemical sensitivity, ecological fragility, and spatial heterogeneity of soils compared with the world's other two concentrated and contiguous karst areas—south-central Europe and eastern North America. These characteristics have led to the serious deterioration of the ecological environment in the area and exposed the area to the dual pressures of population overloading and socio-economic development.(2) From the perspective of the global carbon cycle, the soil carbon pool is an important component of the terrestrial carbon pool. Owing to its unique environment, the source and content of soil organic carbon in the karst area show a high degree of variability under the influence of erosion, land management, and other natural and human factors, making it very difficult to calculate the soil carbon pool in this area.(3)

As the most basic unit of the landform, the slope is the main morphological parameter in the study of the laws of erosion evolution and development. Most of the studies on the soil erosion mechanism on karst slopes start from the factors affecting soil erosion, such as the slope length, slope gradient, and climate.(4) These studies lack a high-precision erosion modulus and do not provide systematic and integral conclusions.(5) This is mainly for two reasons: (1) the special characteristics of geochemical sensitivity and ecological environment vulnerability in the karst area are poorly understood because, for a long time, research methods and soil erosion models for non-karst areas were used, leading to low accuracy and poor regional representativeness of the current erosion modulus data, and (2) the spatial heterogeneity of the soil profile morphology and the physical and chemical properties of this area caused the results obtained by a single-plot runoff method or a nuclide tracer method to poorly reflect the spatial erosion conditions of the whole slope. In addition, the use of general remote sensing methods is disadvantageous at a large spatial scale owing to poor mapping accuracy, absolute positioning difficulty, and other shortcomings.(4)

The ^{137}Cs tracer method has been widely used to study soil erosion.(6) In the study of ^{137}Cs soil erosion on the karst areas of southwest China, the distribution characteristics of ^{137}Cs and their erosive significance in hilly areas and secondary forest have been reported.(7) Moreover, a new ^{137}Cs moving boundary model based on the rainfall and soil erosion characteristics of the karst areas in southwest China has been developed.(8) The Water Erosion Prediction Project (WEPP) model is the only soil erosion prediction model that can describe the spatial distribution of soil erosion on the slope scale.(9) These two methods for slope-scale erosion assessment have been combined in some studies.(10) The WEPP model can only analyze the slope erosion characteristics in 2D space (elevation and slope length) and predict the erosion modulus of individual cross sections from the slope top to toe. The geospatial interface for the WEPP model (GeoWEPP) extends the WEPP model through a remote sensing and Geographic Information System (GIS) spatial analysis module, and can be used to predict the 3D spatial distribution of a watershed using medium- or low-resolution spatial data.(11) GeoWEPP can also evaluate slope-scale erosion based on high-precision spatial data. Combined with the ^{137}Cs moving boundary model method, it can improve the accuracy of erosion assessment at single points and obtain the 3D spatial distribution of erosion, which is a good solution to the two above-mentioned issues of soil erosion assessment in karst areas.

In a karst area, the applicability of the ^{137}Cs tracer method is limited due to scattered shallow soil, underground soil leaks, and a high percentage of bare bedrock.(12) Since the WEPP model currently also has no module to describe underground soil leaks and a high percentage of bare bedrock will affect the soil erodibility parameters, the WEPP simulation results are greater than the measured values.(13) The results show that obvious underground soil leaks and a high percentage of bare bedrock exist in a very rocky desertification area.(14) If the above two methods are applied, it is better to choose a moderately rocky desertification area as the study area and undergo relatively continuous soil mulching, and the applicability of the methods must also be validated.(4)

Toward resolving the above problems, in this study, we selected Zunyi, Guizhou Province, Southwestern China as the investigation area and carried out a short-term and comprehensive soil erosion assessment of the karst slopes of the moderately rocky desertification area using the ^{137}Cs tracer method combined with remote sensing and GIS technology. The research is mainly conducted from the following aspects:(1) We demonstrate the possibility of applying an integrated assessment method to a moderately rocky desertification area by considering the geological environment, soil properties, vegetation cover, and other factors in the investigation area.(2) The ^{137}Cs moving boundary model and the GeoWEPP model based on high-precision digital elevation model (DEM) data are used to improve the time-space resolution and precision of erosion assessment in the investigation area.(3) On the basis of the integrated assessment method, the spatial distribution characteristics and the factors influencing karst slope erosion are studied from a point to the surface and from microscopic to macroscopic scales to perform multidimensional and multiangle research. Starting from an interdisciplinary perspective, we not only provide a new way to assess soil erosion in the especially complex environment of karst areas, but also provide guidelines and a case study to assist international research in this field.

2. Study Area and Methods

2.1 Study area

The investigation area of Zunyi, Guizhou Province [Figs. 1(a) and 1(b)] is located in the middle of the Wujiang River basin, with the mean annual precipitation being about 1000 mm and the mean temperature being 12.6–13.1°C. The proportion of karst landform in this area is 39%, and the area of rocky desertification is less than 10%, which is dominated by a moderately rocky desertification.

The sampling sites are located in two karst slopes A and B [Fig. 1(d)] in Xinpu Town, Zunyi City, with the relative elevation difference of about 50 m and vegetation coverage of more than 80%. The two slopes have different land use types. Slope A is mainly used for orchard and cultivated land, which is significantly affected by human farming activities. Slope B is an uncultivated land, where the age of the trees on the mountain is about 70 years old. The bedrock exposed in this area is continuous dolomite of the Middle-Upper Cambrian Loushanguan Group of neritic facies [Fig. 1(c)], with the total thickness of 1000–1300 m and the overlying red weathering crust thickness of about 7–10 m. The slope distribution is dominated by clay and

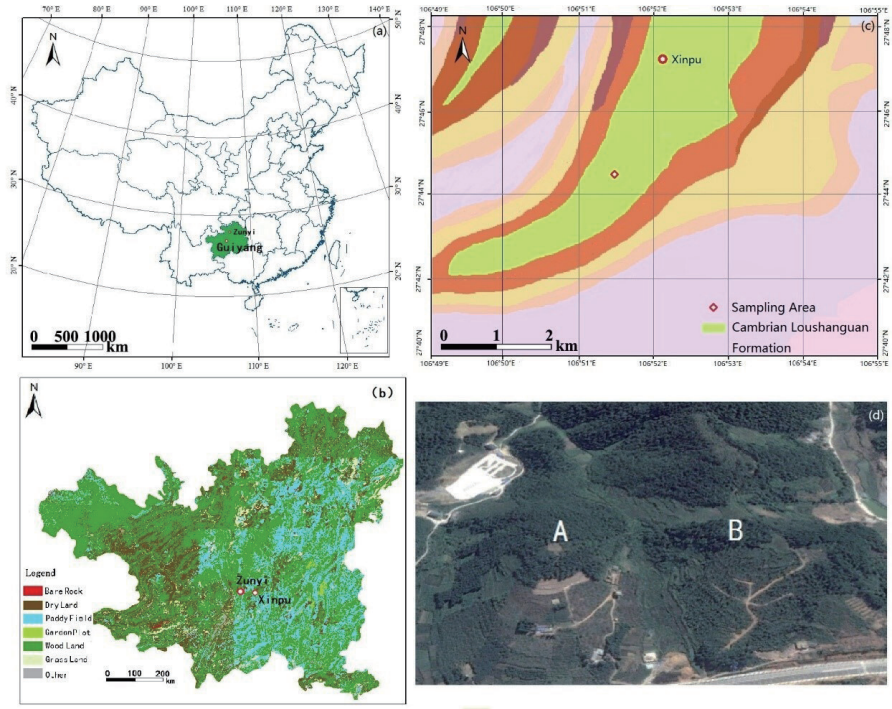

Fig. 1. (Color online) (a) Study area location in Guizhou, China, (b) land use/cover in Zunyi area, (c) geological map of Xinpu, and (d) remote images of study area.

heavy-clay-based continuous thin-layer lime soil that is developed from dolomite parent material weathering. It is gradually thickened from the slope top to toe, which reflects the characteristics of the slope soil erosion–deposition process.

2.2 Physical erosion rate

Undisturbed land erosion models include the empirical model, the profile-shaped model, and the diffusion models.[15] Although both the profile-shaped model and diffusion models were established on the basis of the principle of ^{137}Cs redistribution, the design of the diffusion model is more comprehensive than that of the profile-shaped model. The two best known diffusion models are the transport model and the simplified transport model.[15] The transport model has been used to fully evaluate multiple stages of ^{137}Cs redistribution. However, this model has a complex structure and a relatively large number of parameters that make it difficult to use in practical applications. However, the simplified transport model integrates previous research findings, and by ignoring the convective term in the diffusion equation, the calculation is simplified, and the application of this model is much improved:

$$A_{rm(T)} = A_{ref(T)} \prod_{i=1}^{T} erfc\left[\frac{H}{2\sqrt{Di}}\right], \tag{1}$$

where $A_{rm(T)}$ is the remaining ^{137}Cs inventory in the profile in the sampling year (mBq cm^{-2}), $A_{ref(T)}$ is the ^{137}Cs inventory in the reference profile (mBq cm^{-2}), T is the time from 1963 (a), H is the annual soil loss depth during the period from 1963 to the sampling year (cm), D is the diffusion coefficient (cm^{-2} a^{-1}), and *erfc* is the error function.

The simplified transport model assumes that erosion occurs during the last period at the end of each year; this assumption is suitable for arid areas such as northwest China. These regions have little annual rainfall, which occurs mainly during the short rainy season, which is about one or two months long. For the regions that have long rainy seasons or otherwise abundant rainfall, this assumption no longer corresponds to the actual situation. Examples include most of southern China that has a rainy season lasting over six months. For these areas, the researcher must consider the effect of the pace of erosion on the long-term diffusion process. If this factor is disregarded, the value of $A_{rm(T)}$ in Eq. (2) becomes larger than its actual value, and the annual soil loss depth is overestimated.

The moving boundary model was applied mainly to the areas with a long rainy season by correcting the simplified transport model derived from the analysis of surface soil ^{137}Cs flux variation under persistent erosion. This model is based on the principle of geochemistry kinetics moving boundary,[8] as in Eq. (2):

$$Arm(T) = Aref(T)\left(erf\left[\frac{u\sqrt{t}}{2\sqrt{D}}\right] - 2e^{\frac{3u^2t}{4D}}\left(erf\left[\frac{u\sqrt{t}}{\sqrt{D}}\right] - 1\right) - 1\right). \quad (2)$$

Here, t is the time from 1963 (a) and u is the erosion rate (cm a^{-1}).

2.3 GeoWEPP model

The WEPP model is a hydraulic erosion prediction software program developed by the United States Department of Agriculture. This model can be used to accurately predict soil hydra-erosion, watershed storm runoff, plant growth, root-layer soil moisture, and evapotranspiration in grassland, cultivated land, and woodland.[16] The WEPP erosion module is used to calculate soil erosion caused by rill erosion and inter-rill erosion along a hillslope based on the steady-state continuous equation:[17]

$$\frac{dG}{dx} = Df + Di, \quad (3)$$

where x is the distance (m) in the downhill direction, G is the transport rate [kg/(s·m)], D_i is the inter-rill erosion rate of runoff [kg/(s·m^2)], and D_f is the inter-rill erosion rate [kg/(s·m^2)].

When the hydraulic shear force is greater than the critical soil shear force and the erosion rate is less than the migration ability of the overburden material, the erosion rate of the slope is attributable to only the stripping of the pure soil, which is used for the calculation of rill.

$$Df = Dc\left(1 - \frac{G}{Tc}\right) \tag{4}$$

Here, D_c indicates the separation ability of the rill flow [kg/(s·m^2)], and T_c is the transport capacity of the rill flow [kg/(s·m^2)].

When the transport rate G is greater than the sediment transport capacity of rill runoff, the rill is dominated by erosion and deposition, with the erosion rate being negative and the equation becomes

$$Df = \frac{\beta Vf}{q}(Tc - G), \tag{5}$$

where V_f represents the effective rate of descent of sediment (m/s), q is the unit width flow (m^2/s), and β is the disturbance coefficient of raindrop splash, which is usually 0.5.

From the predicted spatial scale, the WEPP is divided into Hillslope version, Watershed version, and Grid version. Currently, the Hillslope and Watershed versions have been developed and widely used in many areas of the world, but the Grid version has not been completed yet.[18]

The input file of the WEPP Hillslope version mainly includes weather files, slope data files, soil data files, and crop-interrelated files (Fig. 2). Meteorological data can be generated by the CLIGEN modeler.[19] WEPP can produce and output the results of different types and different precisions, the most basic results of which include the main information of runoff and erosion.[19] The simulated results obtained from the WEPP Hillslope version are erosion–deposition information on the cross section of the profile from the slope top to the slope foot. In the case of simulating the erosion information on the entire hillslope space, GeoWEPP is needed. GeoWEPP

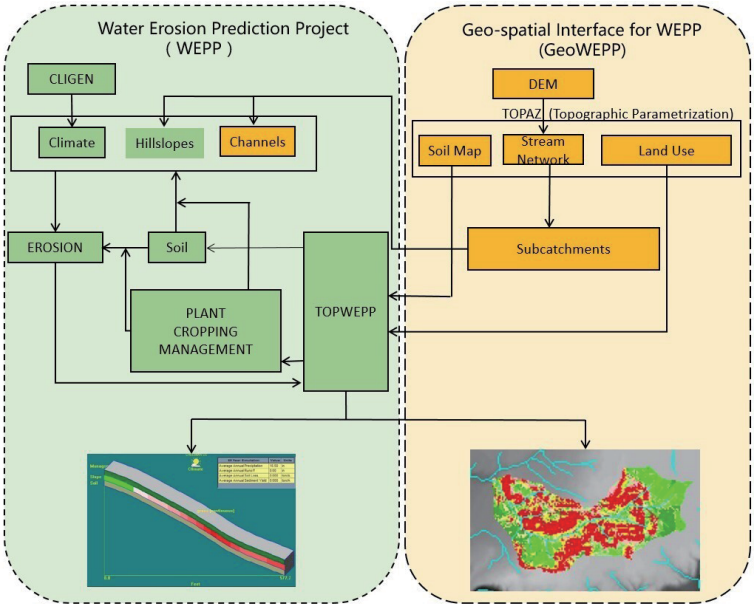

Fig. 2. (Color online) Run process of WEPP and GeoWEPP.

takes the desktop version ArcGIS and its spatial analysis module as the platform, and combines the WEPP model to predict soil erosion at the watershed scale.[19]

GeoWEPP mainly consists of three parts, namely, ArcView, TOPAZ, and TOPWEPP (Fig. 2). First of all, create a watershed DEM and land use and soil properties map with ArcView, input it into GeoWEPP, analyze and process the DEM data with TOPAZ module to draw the watershed concentration grid chart, and then analyze the land use, soil map, and DEM with the spatial overlay analysis function to generate the most basic unit of watershed concentration—subcatchments. Finally, the soil and vegetation parameters of each subcatchment are input into TOPWEPP to output the simulated results.[20]

3. Sampling and Data Sources

3.1 Sampling

3.1.1 ^{137}Cs sampling

Soil samples were collected in the investigation area in April 2014. Sampling lines were laid on two hillslopes, each of which is about 120 m long. A ^{137}Cs sampling point was set every 30 m from the slope top to toe. As shown in Fig. 3, a total of nine profiles were collected, including eight profiles from the two hillslopes and one profile from the valley. To accurately identify the existence of underground soil leak phenomenon on the slope, all sampling sites were stratified. The stratified samples were stripped layer by layer with a blade in the area of 10 × 10 cm at intervals of 2 cm and in the depth of about 30 cm. A total of 135 samples were collected in nine profiles.

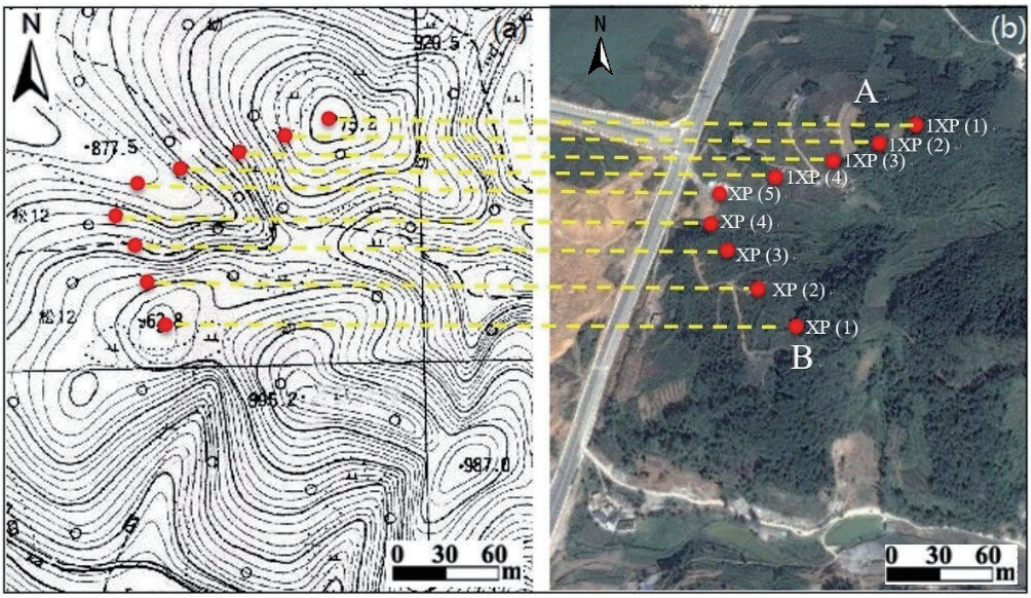

Fig. 3. (Color online) ^{137}Cs sampling sites shown in the (a) topographic map and (b) remote images.

3.1.2 ^{137}Cs test

The samples were weighed indoors after drying and then ground to 0.15 mm size for analysis. The United States CanBerra company's S-100 series 16384 multi-channel analyzer was used for the analysis of ^{137}Cs specific activity, and SAMPO-90 software was used for data processing. Each sample was measured twice with the measurement time of 30000 s each time. If the measurement error was more than 15%, a retest was needed. The results of the laboratory measurement were unit-mass-based ^{137}Cs activity (Bq/g), which, after multiplying the soil bulk density and thickness, could be converted to area-based activity in units of Bq/m^2. The ^{137}Cs inventory (Bq/m^2) refers to the sum of the precipitated ^{137}Cs in all soil layers from the soil surface to the depth where ^{137}Cs is completely undetectable.

$$CPI = \sum_{i=1}^{n} 10^3 * C_i * B_i * D_i \tag{6}$$

Here, CPI (^{137}Cs Point Inventory) is ^{137}Cs inventory of the sampling point, i is the serial number, n is the number of sampling layers, C_i is the mass activity (Bq/g) of ^{137}Cs in the ith sample layer, B_i is the soil bulk density (g/cm^3) of the ith sample layer, and D_i is the thickness (cm) of the ith sample layer.

3.1.3 ^{137}Cs reference

Five soil profiles collected at sites near the nine sampling sites that showed little evidence of physical or biological disturbance of the surface were used as reference soil sites for determining the ^{137}Cs input for the area. The mean ^{137}Cs inventory in these samples was 960 Bq/m^2. Here, it was assumed that this ^{137}Cs inventory (960 Bq/m^2) represented the ^{137}Cs input to the catchment, and we used it as the reference inventory in the moving boundary model to calculate soil erosion rates.[8]

3.2 Data sources

3.2.1 DEM data

The DEM data used with the GeoWEPP model must meet certain precision requirements so that the GeoWEPP model prediction results and the ^{137}Cs moving boundary model estimation results could achieve point-to-point validation. Each sampling site in the investigation area is at intervals of 30 m, so the spatial resolution of the DEM data should be less than 30 m. With the digital topographic map (1:10000) in Xinpu Town [Fig. 4(a)] as the data source, we used ArcGIS10.1 for DEM data extraction in this study to generate 2.5-m high-resolution DEM data. The data quality met the above requirements, as shown in Fig. 4(b).

3.2.2 Land use data

Land use data were sourced from the investigation area on Google Maps in 2014 with the resolution of 1 m. After downloading, stitching, and manual interpretation, it was finally made into a land use map. Land types are divided into six categories, namely, commercial land, bare land, forest land, shrub land, orchard, and cultivated crop, as shown in Fig. 5.

3.2.3 Soil data

The soil properties include five basic attributes of layered soil (sand content, clay content, organic matter content, cation exchange capacity, and gravel content) and six erosion characteristics. The five basic attributes of layered soil are provided by the China Soil Database

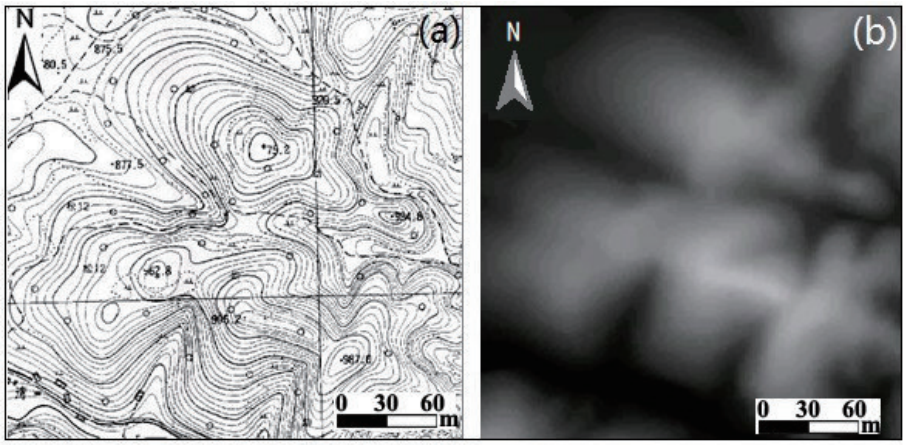

Fig. 4. (a) Topographic map and (b) DEM of study area.

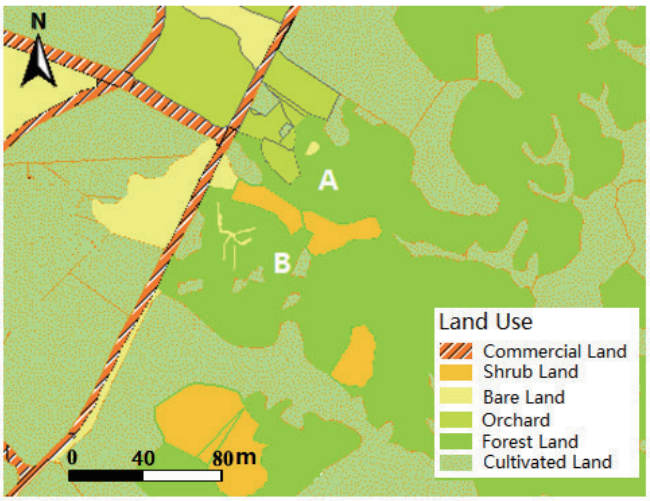

Fig. 5. (Color online) Land use map of study area.

(http://vdb3.soil.csdb.cn/) established by the Institute of Soil Science, Chinese Academy of Sciences. Table 1 shows the basic parameters.

The six erosion characteristics include soil reflectance, saturation, inter-rill erodibility, rill erodibility, critical shear for cropland soil, and effective hydraulic conductivity. These six characteristics can be calculated by inputting the previous five basic attributes into the correlation model, as shown in Table 2.

3.2.4 Climatic data

The climatic file is the most complex in the GeoWEPP model, whose principal factors are rainfall and temperature data. Climatic files need to be input on a daily basis, and the climate generator CLIGEN or breakpoint climate generator BPCDG provided by WEPP can be used for meteorological data simulation. The climatic data in this paper are sourced from the rainfall and temperature data of the Zunyi site in 1963–2010 recorded in the China Meteorological Data Service Center (http://data.cma.cn/site/index.html), as shown in Fig. 6.

The monthly mean values of climate in nearly 50 years were obtained from the data calculation in Fig. 6, as shown in Fig. 7. Daily climatic files of nearly 50 years were obtained by inputting the data into the climate simulator.

4. Results and Discussion

4.1 ^{137}Cs specific areal activity

Figure 8 shows the distribution of ^{137}Cs concentrations of nine profiles in the study area. By comparing and analyzing the changing curves of ^{137}Cs concentration for the nine profiles shown in Fig. 8, the following can be concluded: (1) in uncultivated land profiles except 1XP(1), ^{137}Cs is

Table 1
Main characteristic parameters of soil.

Layer	Depth (mm)	Sand (%)	Clay (%)	Organic (%)	CEC (mmol/100g)	Gravel (%)
A	140	13.5	50	5.13	22.4	0
AC	360	12.8	59.5	2.13	20	0
C	500	9	67.2	0.9	15	0

Table 2
Erosion characteristic parameters of soil.

Parameter	Value	Unit
Soil reflectance	0.58	%
Saturation	0.75	%
Inter-rill erodibility	1.11E+05	kg.s/m^4
Rill erodibility	0.0069	s/m
Critical shear for cropland soil	3.5	Pa
Effective hydraulic conductivity	0.0224	%

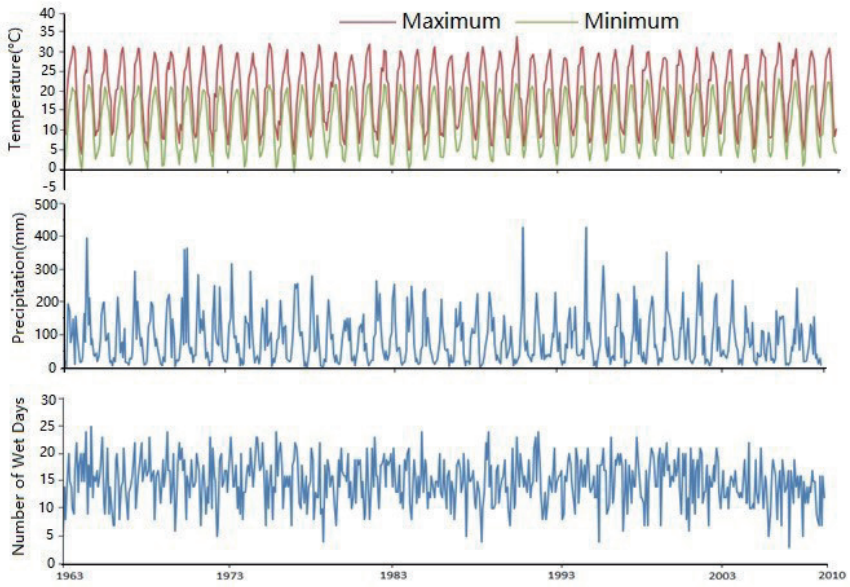

Fig. 6. (Color online) Zunyi monthly (1963–2010) means of maximum/minimum temperature (°C), precipitation (mm), and number of wet days (d) (arranged from top to bottom).

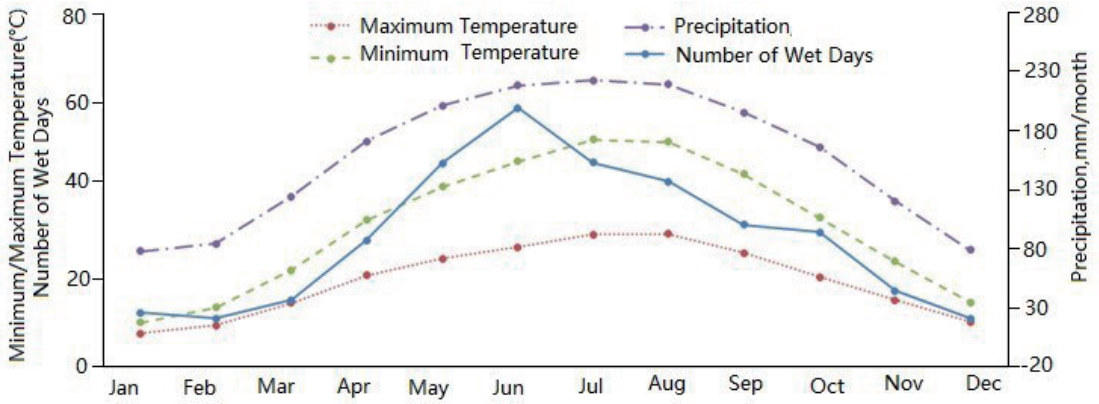

Fig. 7. (Color online) Zunyi monthly (1963–2010) means of precipitation (mm), maximum/minimum temperature (°C), and number of wet days.

seen in the topsoil layer of 0–6 cm. However, in cultivated land profiles, ^{137}Cs primarily exists in the topsoil layer with a depth of 0–20 cm. (2) From the distribution trend of ^{137}Cs concentration in the profiles, the ^{137}Cs concentration of uncultivated profiles except XP(1) decreased exponentially as depth increases, whereas the overall distribution trend of cultivated profiles except 1XP(4) was relatively uniform. These analyses indicated that XP(1), 1XP(1), and 1XP(4) were somewhat special, differing from other profiles in the same group. Although XP(1) was an uncultivated site, the ^{137}Cs distribution depth was larger than 6 cm, which may indicate that it was affected by human cultivation a few decades earlier. XP(1) showed strong leaching of this

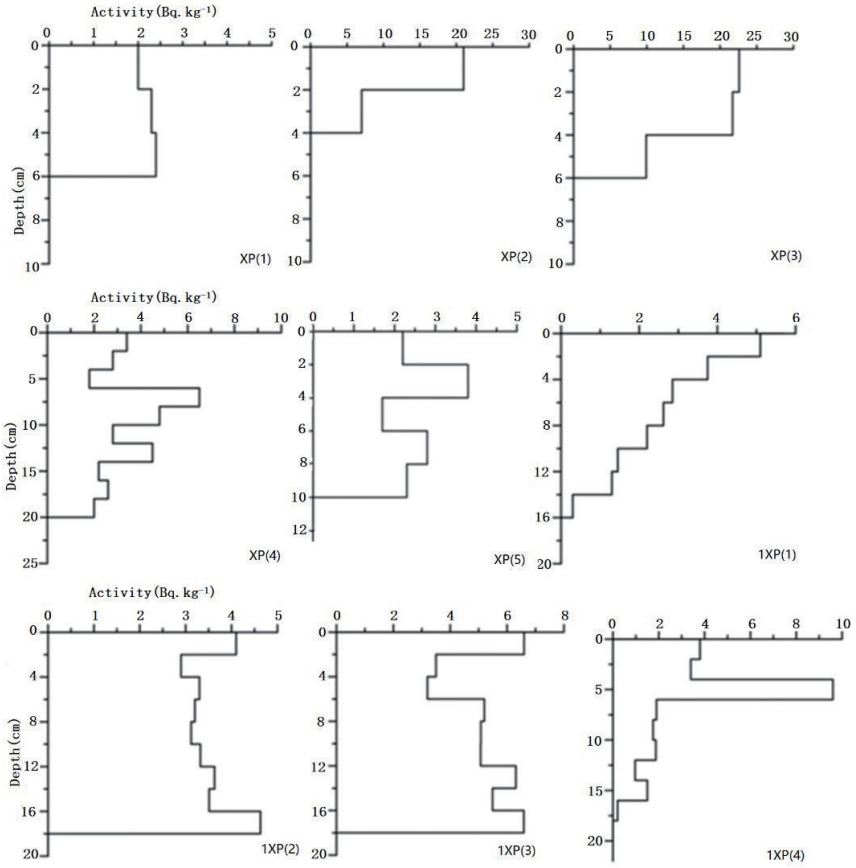

Fig. 8. Distribution of ^{137}Cs concentrations of nine profiles.

profile, which caused a higher infiltration rate than the diffusion rate, so that the concentration in the lower part of the profile is higher than that in the upper part. XP(4) was located at the foot of the slope, an area that may have been deeply affected by human cultivation. It is a very clear trend that ^{137}Cs enrichment occurs in the topsoil, consistent with the theory that different types of crops and fertilization have influences on the adsorption and enrichment of ^{137}Cs. The ^{137}Cs distribution in the cultivated land is heavily influenced by cultivation and field management, whereas most areas in the Loess Plateau are flat with mechanized farming. However, because the area investigated in this paper is located in hilly land, hand cultivation is used, and the soil was not disturbed to as great a depth, with a smaller ^{137}Cs distribution depth than in mechanized farming.

4.2 Feasibility of ^{137}Cs method in karst terrain

We considered it improper to use the ^{137}Cs tracer technique to evaluate the slope soil erosion in karst areas for three major reasons: (1) soil grains in karst sloping fields are coarse, fine soils (<2 mm) make up an average of only 24.8%, the soil layer is thin, the total amount of ^{137}Cs absorption is limited, and the average areal activity of ^{137}Cs as measured in related works is only

260 Bq/m^2; (2) the fraction of loose surface stones in sloping karst fields is high, and some of the ^{137}Cs that falls onto loose stones along with rainfall are directly washed away with runoff without being absorbed by the soil; (3) observation and analysis of the creep phenomenon in karst soils showed that a pure carbonate rocky mountain can be considered a stone sieve full of holes. The soil in these areas fills the pores and holes created by chemical corrosion, and pipeline erosion occurs below the soil layer. Some of this soil later enters underground channels. As a consequence, soil losses in karst areas are the results of aboveground slope erosion, underground chemical corrosion, and gravitational erosion. However, the ^{137}Cs element tracer technique can only be used in areas in which the major type of erosion is aboveground slope erosion. For other areas, the erosion rate calculated using this method will be larger than the actual value.

In the area investigated in this paper, the clay particle content of the soil was relatively high (≈58.6%).[21] Moreover, both the geomorphology and soil showed relatively good ^{137}Cs adsorption conditions, with the average ^{137}Cs areal activity of nine sampling profiles over 875 Bq/m^2, whereas it was 960 Bq/m^2 in the reference profile. For both sloping fields, the ^{137}Cs specific areal activity showed a gradual increasing trend from the hilltop to the foot, indicating slope erosion in the investigated fields. Whether there was any underground soil loss in the investigated area can be determined by examining the distribution of the ^{137}Cs concentration in the profiles. After studying the underground soil loss in karst sloping fields, Wei *et al*. reported that the ^{137}Cs concentration showed a sharp increase at the bottom of the profiles where there was underground loss.[12] However, in all the profiles investigated in this paper, no similar conditions were observed.

It is generally believed that the ^{137}Cs tracer is not suitable for soil erosion assessment in a very rocky desertification area such as Puding and Pingba in Guizhou where underground soil leaks have a strong correlation with rock fissure.[14] Thus, moderately rocky desertification areas were chosen for soil erosion assessment with ^{137}Cs.[16] The Zunyi area is not a high-incidence area of rocky desertification, where the rocky desertification rate is less than 10%, and the vegetation coverage of the investigation area is 80%. To sum up, it is considered that no underground soil leaks exist in the surface soil of karst in moderately rocky desertification areas, and the ^{137}Cs tracer is suitable for soil erosion research in these areas.

4.3 Evaluation of soil erosion

The nine sampling sites include six erosion sites and three deposition sites. The erosion and deposition rates for each site were determined by utilizing the model of ^{137}Cs moving boundaries (Table 3). Soil erosion is graded in reference to SL190-2007 criteria.

In Table 3, there were four moderate erosion sites, two micro-degree erosion sites, and three deposition sites among the nine sampling sites, which indicated that the overall soil and water conservation in the investigation area was good. In general, the soil erosion modulus of cultivated land in the same area was higher than that of uncultivated land, but the average soil erosion modulus of cultivated land slope A in the investigation area was smaller than that of uncultivated land slope B, which may be related to the local work of transforming a sloping farmland into a terraced field for soil and water conservation in the early stage. According to the

Table 3
Conditions of soil erosion of sampling points.

Sampling points	Erosion modulus ($t \cdot km^{-2} \cdot a^{-1}$)	Erosion intensity
XP(1)	1911	Moderate
XP(2)	130	Micro-degree
XP(3)	−520	Deposition
XP(4)	−39	Deposition
XP(5)	949	Moderate
1XP(1)	247	Moderate
1XP(2)	−390	Deposition
1XP(3)	9	Micro-degree
1XP(4)	234	Moderate

literature, the earliest project of transforming a slope into a terrace in Zunyi began in 1991.[22] From the implementation effect, the slope gradient was reduced and the slope length was also greatly reduced after transforming a slope into a terrace, thus effectively preventing soil erosion on the cultivated land slope.

According to existing knowledge, there are three main ways of weathering the carbonate rocks in the Wujiang River basin: in situ weathering, in situ erosion and weathering, and use of fluid carrying accumulation soil.[13] Figure 9 shows the relationship between soil erosion intensity and elevation. It can be seen that the two slopes have a clear erosion–deposition phenomenon from the slope top to toe, which has strongly supported the above viewpoint. It is also noteworthy that the soil erosion-deposition rate of cultivated land slope A is lower than that of uncultivated land slope B, indicating that human activities with soil and water conservation measures as the main form have changed the erosion, transport, and deposition of sediment in the slope. Human activities may become an important geomorphologic force in this area.

4.4 Spatial variation of soil erosion

On the basis of input parameters, GeoWEPP automatically generates the map for eight levels of soil erosion in the investigation area [Fig. 10(a)]. To analyze the spatial distribution mechanism of slope erosion and factors influencing it, contour lines and DEM data were used respectively to extract TIN data [Fig. 10(b)] and the slope map [Fig. 10(c)].

In Fig. 10(c), with a small slope gradient (≤17°) and flat terrain, the top of the two slopes is dominated by micro-degree and moderate erosion. In the initial formation stage of water flow on a slope, the site has slow ground runoff and weak rain erosion ability. The runoff of slopes A and B [Fig. 10(a)] can be roughly divided into two directions along the slope direction: yellow arrow and white arrow [Fig. 10(b)]. The yellow arrow direction shows a small slope length, a steep slope gradient, and a high speed of surface runoff, which is prone to generate a strong slope erosion; the white arrow direction shows a large slope length and a gentle slope gradient, which is easy to form a deposition area at Sites D_1 and D_2 [Fig. 10(a)] at the slope toe. Owing to the gentle slope gradient at the bottom of the two slopes, the runoff from the two slopes forms a

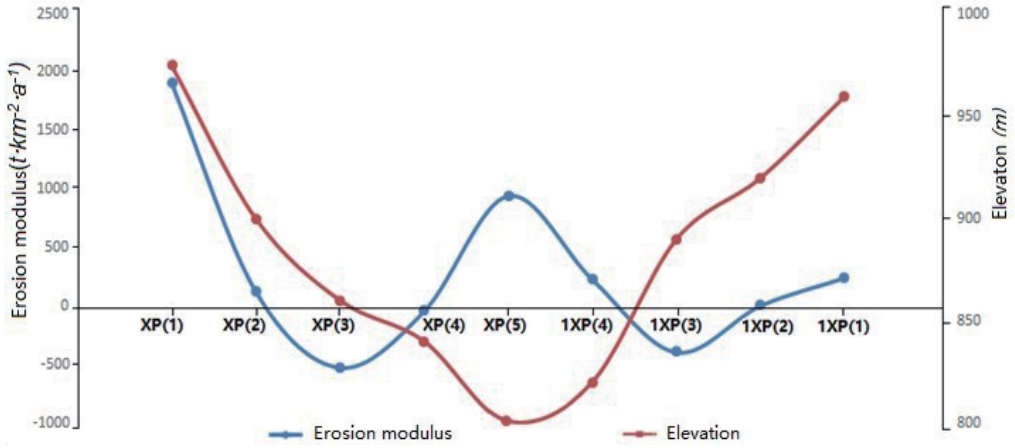

Fig. 9. (Color online) Variation of erosion–deposition modulus of sampling sites at different slope positions.

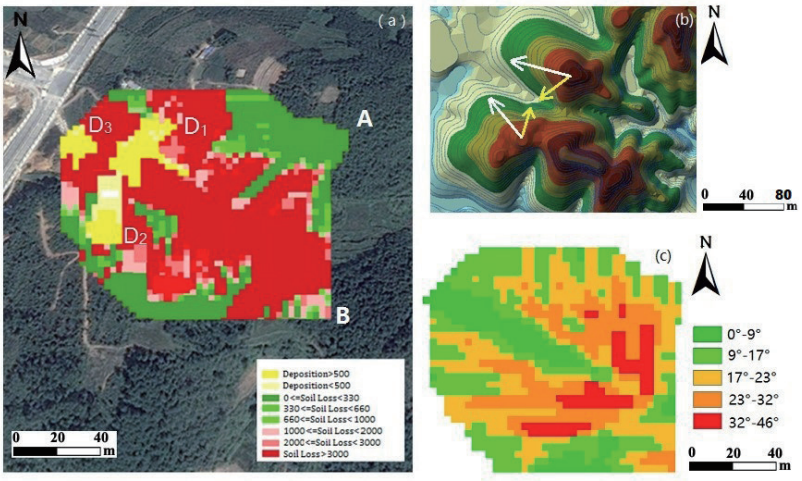

Fig. 10. (Color online) (a) Soil loss map, (b) TIN map, and (c) slope map.

catchment area here where the runoff quantity and erosion intensity are large and gully erosion is prone to occur. Site D_3 [Fig. 10(a)] is a sediment deposition area, which is mainly due to its low terrain.

To study the relationship between slope and erosion, the area ratio (AR for short), erosion contribution ratio (ER for short), deposition contribution ratio (DR for short), and erosion area ratio (EAR for short) of each slope were calculated, as shown in Table 4.

In Table 4, AR is 79.5% and ER is 80.9% within the slope gradients of 9–32° slope bands. EAR increases gradually with the increase in the slope gradient and has no deposition in the slope gradients of 32–46° slope bands, whereas AR is 71.8% and DR is 93.8% within the slope gradients of 0–23° slope bands. It is worth noting that AR, ER, and DR are the largest within the range of 17–23° slope bands, indicating that this slope gradient range has a greater effect than other four slope ranges on the deposition and erosion processes throughout the region.

Table 4
Soil erosion conditions in different slope grades.

Slope	*AR* (%)	*ER* (%)	*DR* (%)	*EAR* (%)
0–9°	12.7	10.7	29.0	75.5
9–17°	27.2	26.8	31.9	88.5
17–23°	31.9	32.2	32.9	90.2
23–32°	20.4	21.9	6.2	98.5
32–46°	7.8	8.4	0	100

Note: $AR = \frac{Area\ of\ a\ slope}{Total\ area}$, $ER = \frac{Erosion\ area\ of\ a\ slope}{Total\ erosion\ area}$, $DR = \frac{Deposition\ area\ of\ a\ slope}{Total\ deposition\ area}$, $EAR = \frac{Erosion\ area\ of\ a\ slope}{Area\ of\ a\ slope}$.

4.5 GeoWEPP model validation

GeoWEPP is available for the automatic grading of erosion modulus through the system module. Only the range of erosion modulus rather than the exact value can be obtained at each point. By comparing the value estimated with the ^{137}Cs moving boundary model (CE for short) with that predicted with the GeoWEPP model (GP for short) at each sampling site, it is considered that the GP is accurate if the CE is located within the scope of the GP, as shown in Table 5.

In Table 5, the GP of the sampling sites on the uncultivated land was accurate. The GP of the sampling sites on the cultivated land was significantly higher than the CE. Overall, the GeoWEPP model erosion prediction results of the sampling sites on uncultivated land were significantly better than those of the sampling sites on cultivated land.

The main factors that limit the use of the GeoWEPP model in the karst area are also underground soil leaks and high percentage of bare bedrocks.[23] The relevant argument in Sect. 4.2 provides a prerequisite for applying the GeoWEPP model to the investigation area. To correspond to the ^{137}Cs tracer erosion assessment, the GeoWEPP model simulation time is set to be 50 years. The related research shows that the larger the scale of the GeoWEPP model simulation time, the higher the precision.[23] Therefore, the GP has a good accuracy on the uncultivated land. The GP of the cultivated land is significantly higher than the CE, which may be related to transforming a slope into a terrace. The trapping of sediment by a terrace field mainly depends on the ridge construction. However, it is difficult to use the current GeoWEPP model to simulate the terraced field, which results in the prediction result being larger than the measured value.[24]

In conclusion, it is considered that the GeoWEPP model is suitable for the short-term erosion prediction of uncultivated land in a karst moderately rocky desertification area, but it yields a remarkable error in the prediction of soil erosion in cultivated land. Thus, in the next step, the model needs to be modified and debugged to improve the simulation precision.

Table 5
GeoWEPP model verification.

Sampling points	Land use	*CE* ($t \cdot km^{-2} \cdot a^{-1}$)	*GP* ($t \cdot km^{-2} \cdot a^{-1}$)	Accuracy
XP(1)	Uncultivated land	1911	[1000,2000]	Yes
XP(2)	Uncultivated land	130	[0,330]	Yes
XP(3)	Uncultivated land	−520	<−500	Yes
XP(4)	Uncultivated land	−39	[0,−500]	Yes
XP(5)	Cultivated land	949	>3000	No
1XP(1)	Uncultivated land	234	[0, 330]	Yes
1XP(2)	Uncultivated land	9	[0, 330]	Yes
1XP(3)	Cultivated land	−390	>3000	No
1XP(4)	Cultivated land	247	>3000	No

5. Conclusions

In this paper, we selected typical karst slopes of a moderately rocky desertification area in Zunyi, Guizhou Province as the research subject, where the geological environment, soil properties, and vegetation cover conditions are favorable for the adsorption of ^{137}Cs. The average ^{137}Cs areal activity of nine sampling sites is 875 Bq/m^2 (background value is 960 Bq/m^2). The depth variation characteristics of ^{137}Cs concentration of all sampling sites' profiles indicate no underground soil leaks existing in the surface soil, which proves the feasibility of using the ^{137}Cs tracer method for soil erosion assessment in the karst moderately rocky desertification area and provides a prerequisite for the application of the GeoWEPP model.

The soil erosion intensity in the investigation area is dominated by micro-degree and moderate erosion. The average soil erosion rate of uncultivated land is higher than that of cultivated land, which may be related to the active water and soil conservation in the area. From the perspective of the circulation of the earth's surface in karst, an apparent soil erosion–deposition phenomenon exists in the two slopes from the slope top to toe, which strongly supports the theory of lime soil formation in this area. It is also noteworthy that the erosion–deposition is stronger in cultivated land than in uncultivated land, indicating that human activities with soil and water conservation measures have changed the erosion, transport, and deposition processes and may become an important geomorphologic force in this area in the short term.

The spatial distribution characteristics of soil erosion in the investigation area are obtained by using remote sensing and GIS technology based on high-precision DEM data. The soil erosion intensity of a slope top is relatively weak, whereas that of a steep slope increases from the slope top to toe. Deposition is prone to occur at the slow slope toe. The slope is also the most important factor that causes different spatial and temporal distributions of soil erosion. The band with the slope of 17–23° is the main erosion and deposition slope section in the study area.

The results show that the GeoWEPP model for soil erosion prediction is more suitable for uncultivated land in the karst moderately rocky desertification area than for cultivated land where the prediction value tends to be larger. In the next step, the selection and adjustment of model parameters need to be optimized to improve the simulation precision in the karst area.

References

1 Prosdocimi, M., A. Cerdà, and P. Tarolli: Catena **141** (2016) 1. https://doi.org/10.1016/j.catena.2016.02.010
2 Y. Li, J. Shao, S. Wang, and C. Wei: Prog. Phys. Geog. **25** (2006) 1. https://doi.org/10.3969/j.issn.1007-6301.2006.05.001
3 C. Liu: Biogeochemical Processex and Cycling of Nutrients in the Earth's Surface: Cycling of Nutriens in Soil-Plant Systems of Karstic Environments, Southest China (Science Press, Beijing, 2006) 1st ed., Chap. 3.
4 K. Krklec, D. Domínguez-Villar, R. M. Carrasco, and J. Pedraza: Geomorphology **264** (2016) 1. https://doi.org/10.1016/j.geomorph.2016.04.007
5 G. Yang, J. Wang, X. Cai, and Y. An: Soil Erosion Evaluation and Numerical Simulation in Karst Area (China Meteorological Press, Beijing, 2013) 1st ed., Chap.2.
6 L. Mabit, S. Chhem-Kieth, P. Dornhofer, A. Toloza, M. Benmansour, C. Bernard, E. Fulajtar, and D. E. Walling: Guidelines for Using Fallout Radionuclides to Assess Erosion and Effectiveness of Soil Conservation Strategies (IAEA publication, Vienna, 2014) 1st ed., Chap. 2.
7 X. Bai, X. Zhang, H. Chen, and Y. He: Land Degrad. Dev. **21** (2010) 474. https://doi.org/10.1002/ldr.983
8 C. Yin and H. Ji: J. Environ. Radioactiv. **150** (2015) 152. https://doi.org/10.1016/j.jenvrad.2015.08.010
9 W. S. Merritt, R. A. Letcher, and A. J. Jakeman: Environ. Modell. Softw. **18** (2003) 761.https://doi.org/10.1016/S1364-8152(03)00078-1
10 Z. Zheng, X. Zhang, and X. He: J. Soil Water Conserv. **2** (2007) 21. https://doi.org/CNKI:SUN:TRQS.0.2007-02-005
11 D. C. Flanagan, J. R. Frankenberger, T. A. Cochrane, C. S. Renschler, and W. J. Elliot: Trans. Am. Soc. Agri. Biol. Eng. **56** (2013) 591. https://doi.org/10.13031/2013.42681
12 X. Wei, D. Yuan, and S. Xie: J. Soil Water Conserv. **6** (2010) 16. https://doi.org/10.13870/j.cnki.stbcxb.2010.06.013
13 M. Z. Long, W. U. Ke-Hua, and K. N. Xiong: Carsologica Sinica **25** (2014) 25. https://doi.org/10.1023/A:1007071527408
14 Y. Tang, X. Zhang, J. Zhou, Y. She, P. Yang, and J. Wang: Carsologica Sinica **2** (2010) 121. https://doi.org/10.3724/SP.J.1011.2010.01385
15 X. Zhang, Y. Long, X. He, J. Fu, and Y. Zhang: J. Environ. Radioact. **99** (2008) 1242. https://doi.org/10.1016/j.jenvrad.2008.03.001
16 D. C. Flanagan, J. R. Frankenberger, T. A. Cochrane, C. S. Renschler, and W. J. Elliot: Trans. Am. Soc. Agri. Biol. Eng. **53** (2013) 1399. https://doi.org/10.1590/S1415-43662010000900015
17 J. M. Laflen, L. J. Lane, and G. R. Foster: J. Soil Water Conserv. **46** (1991) 34. https://doi.org/10.1061/(ASCE)0733-9437(1991)117:1(150.2)
18 X. Yu, F. Qin, J. Li, and M. Zhang: Erosion Dynam. Watershed (Science Press, Beijing, 2007) 1st ed., Chap. 3.
19 J. Boll, E. S. Brooks, B. Crabtree, S. Dun, and T. S. Steenhuis: J. Am. Water Resour. Assoc. **51** (2015) 330. https://doi.org/10.1111/1752-1688.12294
20 V. Yadav and G. P. Malanson: Geomorphology **106** (2009) 304. https://doi.org/10.1016/j.geomorp-h.2008.11.011
21 C. Yin: Weathering Erosion and Elemental Migration in Zunyi Karst Critical Zone, Guizhou (Capital Normal University, Beijing, 2015) Chap. 3.
22 D. Li: Southwest Militia **5** (1995) 16. https://xueshu.baidu.com/usercenter/paper/show?paperid=135ed755e05f43678cbda7bc1830cce7&site=xueshu_se&hitarticle=1
23 M. Z. Long, W. U. Ke-Hua, and K. N. Xiong: Carsologica Sinica **33** (2014) 25. https://xueshu.baidu.com/usercenter/paper/show?paperid=b82857f50c84576a3dd67c68acca6598
24 D. Yan, A. Wen, Z. Zhang, and J. J. Zheng: Earth Env. **5** (2007) 42. https://doi.org/10.3321/j.issn:1009-2242.2007.05.011

About the Authors

Chuan Yin received his B.E. degree from Sichuan Normal University, China, in 2009 and his M.S. and Ph.D. degrees from Capital Normal University, China, in 2012 and 2015, respectively. From 2015 to 2018, he conducted postdoctoral research at the National Geomatics Center of China. Since 2018, he has been a lecturer at Beijing University of Civil Engineering and Architecture. His research interests are in geoscience modeling. (yinchuan@bucea.edu.cn)

Kai Xiong received her B.E. degree from Hebei Normal University, China, in 2013 and her M.S. and Ph.D. degrees from Capital Normal University, China, in 2013 and 2019, respectively. Since 2019, she has been a researcher at the Beijing Municipal Research Institute of Environmental Protection. Her research interests are in environmental remediation. (xiongkai@cee.cn)

Hongbing Ji conducted postdoctoral research at the Institute of Geographical Sciences and Natural Resources Research, Chinese Academy of Sciences, China from 2001 to 2003. From 2003 to 2010, he was a professor at Capital Normal University, China. Since 2010, he has been a professor at the University of Science & Technology Beijing. His research interests are in soil pollution and remediation technology. (ji.hongbing@hotmail.com)

Mingyi Du received his B.E. and M.S. degrees from Liaoning Technical University, China, in 1984 and 1990, respectively, and his Ph.D. degree from China University of Mining & Technology in 2001. From 1984 to 2005, he was an assistant lecturer, then an associate professor at Liaoning Technical University, China. Since 2005, he has been a professor at China University of Mining & Technology. His research interests are in smart cities and the Internet of Things. (dumingyi@bucea.edu.cn)